

# Colour effective particles and confinement

V.V. Anisovich

PNPI, Gatchina 188300, Russia

November 26, 2018

## Abstract

*Talk given at the Workshop "Hadron Structure and QCD", Gatchina, Russia, 3-6 July 2010*

Here I present a brief review of papers where the idea is pushed forward that colour confinement is realized by singular interaction at large distances between colour effective particles (constituent quarks, diquarks, massive effective gluons).

## 1 Constituent quarks as colour effective particles

The first successful steps in understanding the internal structure of hadrons were made in 60's by introducing an idea of constituent quarks, according to which baryons are three-quark systems and mesons are quark-antiquark ones. Non-relativistic description of these systems gave rise to the systematization of low-lying states ( $SU(6)$  symmetry) and allowed one to work with constituent quarks as non-flying out objects due to the potential barrier. The weak point of this approach is its inapplicability to highly excited states. Later on, experimental and theoretical studies revealed more complicated structure of hadrons, constituent quarks being spatially separated clusters of the QCD particles. It allows us to consider the constituent quark as an effective particle, *i.e.* a "dressed quark" of the valence QCD-quark.

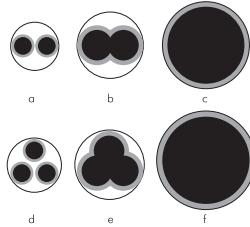


Figure 1: Quark structure of a meson (a–c) and a baryon (d–f) in the constituent quark model. At moderately high energies (a,d) constituent quarks inside the hadron are spatially separated. With the energy growth, quarks overlap partly (b,e); at superhigh energies (c,f) quarks are completely overlapped, and hadron–hadron collisions lose the property of additivity.

For reactions at low and moderately high energies the masses of the light constituent quarks ( $q = u, d, s$ ) are of the order of  $m_u \simeq m_d \simeq 300 - 400$  MeV,  $m_s \simeq 500$  MeV. The size of the light constituent quark  $\langle r_{\text{constituent quark}}^2 \rangle \simeq 0.1 \text{ fm}^2$ .

## 2 Systematization of mesons in terms of constituent quarks

The systematization of mesons support the idea of constituent quarks. A decade ago, considerable progress was reached in the determination of highly excited meson states in the mass region 1950–2400 MeV. These results allowed us to systematize  $q\bar{q}$ -meson states on the  $(n, M^2)$  and  $(J, M^2)$  planes,  $n$  being the radial quantum number of a  $q\bar{q}$  system with mass  $M$  and spin  $J$ . The  $q\bar{q}$  states,  $n^{2S+1}L_J q\bar{q}$ , fill in the following  $(n, M^2)$  trajectories:

$$\begin{aligned}
^1S_0 &\rightarrow \pi(10^{-+}), \eta(00^{-+}) ; \\
^3S_1 &\rightarrow \rho(11^{--}), \omega(01^{--})/\phi(01^{--}) ; \\
^1P_1 &\rightarrow b_1(11^{+-}), h_1(01^{+-}) ; \\
^3P_J &\rightarrow a_J(1J^{++}), f_J(0J^{++}), J = 0, 1, 2 ; \\
^1D_2 &\rightarrow \pi_2(12^{-+}), \eta_2(02^{-+}) ; \\
^3D_J &\rightarrow \rho_J(1J^{--}), \omega_J(0J^{--})/\phi_J(0J^{--}), J = 1, 2, 3 ; \\
^1F_3 &\rightarrow b_3(13^{+-}), h_3(03^{+-}) ; \\
^3F_J &\rightarrow a_J(1J^{++}), f_J(0J^{++}), J = 2, 3, 4 .
\end{aligned} \tag{1}$$

Trajectories for ( $C = -$ ) meson states on the  $(n, M^2)$  plane are shown in Figs. 2, 3, 4.

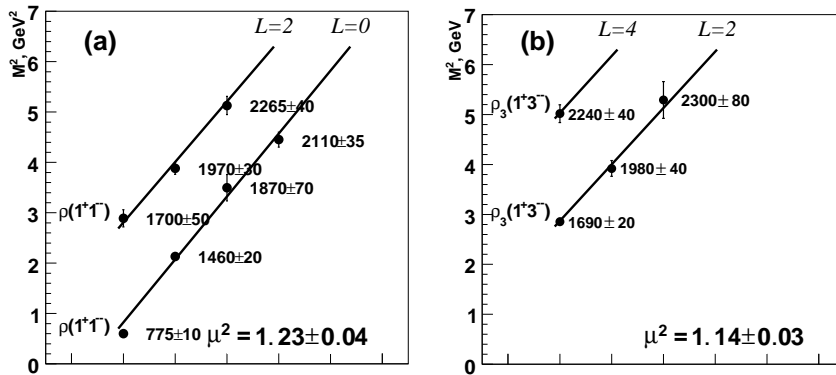


Figure 2: Trajectories for ( $C = -$ ) meson states on the  $(n, M^2)$  plane. The black dots mark the observed states, open circles stand for the predicted states. For mesons, the used notation is  $(I^G J^P)$ .

Recall that  $L$  refers to the quark notation of state:  $n^{2S+1}L_J q\bar{q}$ . Linear trajectories give the  $n^{2S+1}L_J q\bar{q}$  states:

$$M^2 = M_0^2 + (n - 1)\mu^2, \tag{2}$$

where  $M_0$  is the mass of the basic state,  $n = 1$ . The slope  $\mu^2$  is of the same order for the all trajectories.

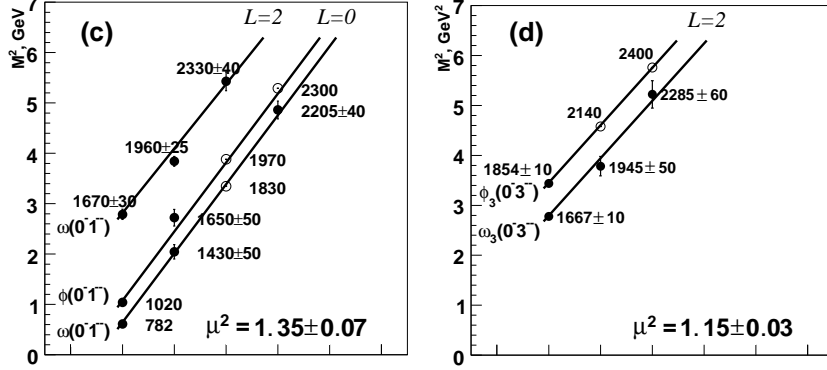


Figure 3: Trajectories for ( $C = -$ ) meson states. Isoscalar states have two flavour components each,  $n\bar{n} = (u\bar{u} + d\bar{d})/\sqrt{2}$  and  $s\bar{s}$ , this doubles the number of trajectories.

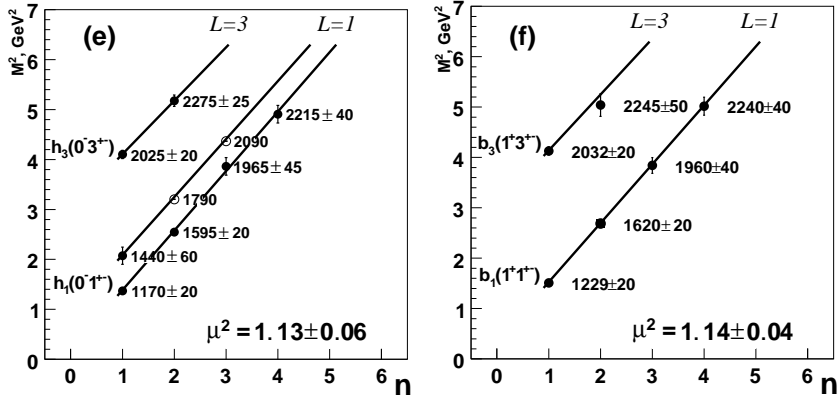


Figure 4: Trajectories for ( $C = -$ ) meson states. States with  $J = L \pm 1$  have two components: at fixed  $J$  there are states with  $L - 1$  and  $L + 1$ , so one may assert the doubling of trajectories at fixed  $J$ , for example, for  $(1, 1^{--})$  and  $(1, 3^{--})$ .

The linearity of  $(n, M^2)$  trajectories at  $M \lesssim 2.4$  GeV with the universal slope  $\mu^2 \simeq 1.15$   $\text{GeV}^2$  was observed in [2] – in the region of large masses it was essentially based on meson spectra analyses in the  $p\bar{p}$  annihilation [3], partial wave analysis of  $\pi^+\pi^-\pi^0$  production in two-photon collisions at LEP [4] and simultaneous  $K$ -matrix fit of a number of meson spectra [5]. Recently performed  $K$ -matrix analyses [6] confirm the linearity of trajectories.

In Fig. 5, one can see states,  $f_0(1200 - 1400)$  and  $f_2(2000)$ , which are extra for the  $q\bar{q}$  systematics. They are glueballs: scalar [7, 8] and tensor [9] ones (hadronic decays tell us that  $f_0(1200 - 1400)$  and  $f_2(2000)$  are nearly flavour singlet).

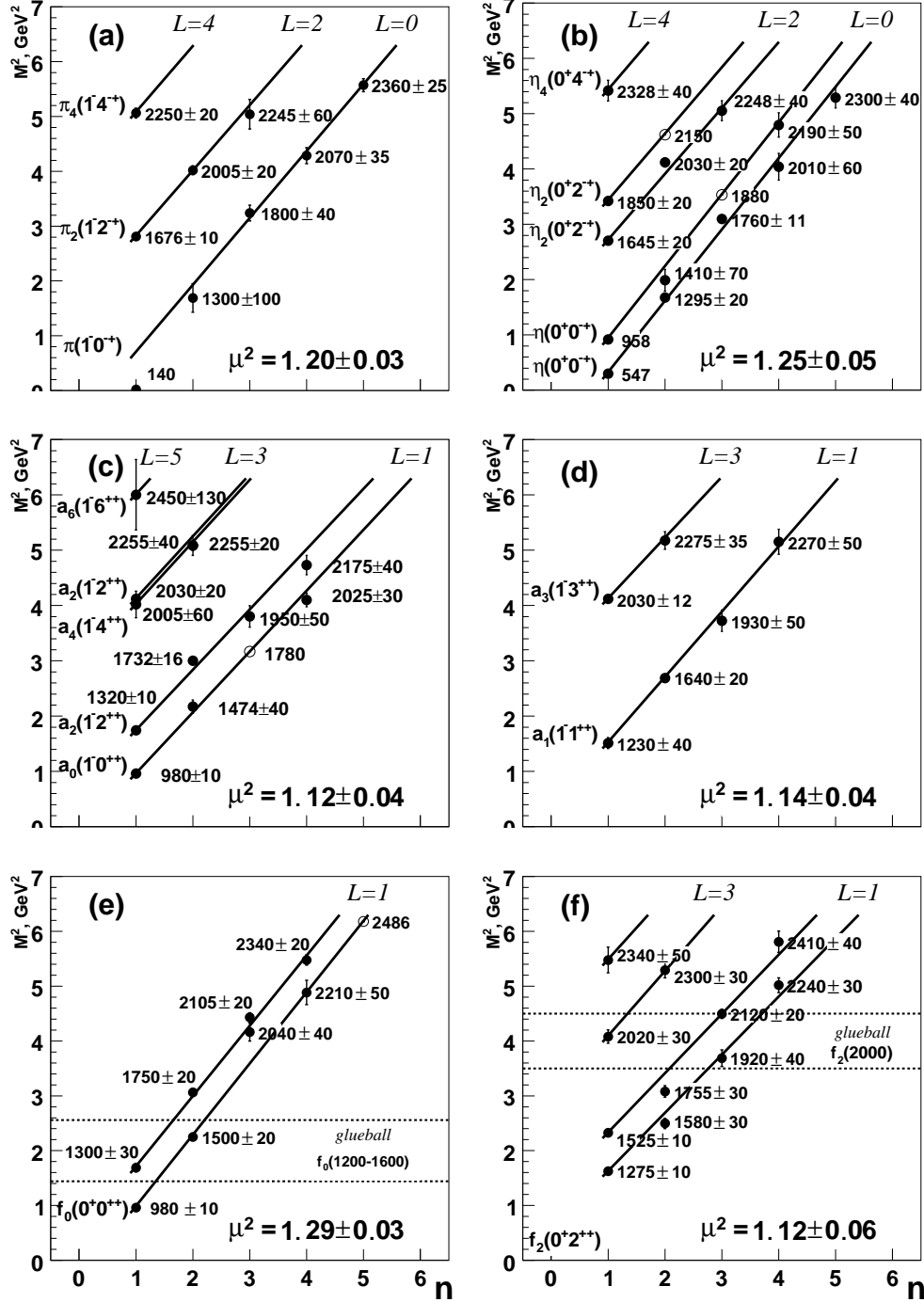


Figure 5: Trajectories for  $(C = +)$  meson states on the  $(n, M^2)$  planes. Dotted lines show mass regions of the scalar ( $f_0(1200 - 1600)$ ) and tensor ( $f_2(2000)$ ) glueballs. With the trajectories on  $(n, M^2)$  plots, one can easily draw the  $(J, M^2)$  ones (Chew-Frautschi trajectories).

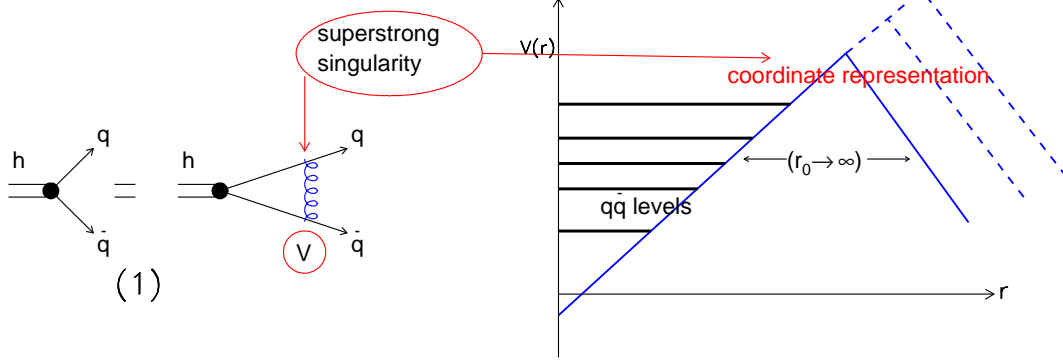


Figure 6: Example which shows how in quantum mechanics (the Schrödinger equation is drawn in the left-hand side of the figure) one may prevent quarks to leave the confinement trap by introducing for the  $q\bar{q}$  system a barrier at  $r \sim r_{hadron}$  (the right-hand side of the figure).

### 3 Spectral integral equation for $q\bar{q}$ mesons and confinement

In low-energy physics we can work with constituent quarks as with standard particles but taking into account their confinement. Quantum mechanics, see Fig. 6, show the way to prevent quarks to leave the confinement trap: for the  $q\bar{q}$  system one should introduce a barrier at  $r \sim r_{hadron}$ .

The relativistic generalization of the calculation technique was performed in terms of the dispersion relation method [10] – correspondingly, for  $b\bar{b}$ ,  $c\bar{c}$  and  $q\bar{q}$  mesons.

#### 3.1 Calculation results for $q\bar{q}$ mesons: masses and wave functions

In the  $q\bar{q}$  sector, by fitting to the interaction, there were found wave functions and mass values of mesons lying on the following  $(n, M^2)$  trajectories:

$$\begin{aligned}
 L = 0 & : \quad \pi(0^{-+}), \rho(1^{--}), \omega(1^{--}), \phi(1^{--}), \\
 L = 1 & : \quad a_0(0^{++}), a_1(1^{++}), a_2(2^{++}), b_1(1^{+-}), f_2(2^{++}), \\
 L = 2 & : \quad \pi_2(2^{-+}), \rho(1^{--}), \rho_3(3^{--}), \omega(1^{--}), \omega_3(3^{--}), \phi_3(3^{--}), \\
 L = 3 & : \quad a_2(2^{++}), a_3(3^{++}), a_4(4^{++}), b_3(3^{+-}), f_2(2^{++}), f_4(4^{++}), \\
 L = 4 & : \quad \rho_3(3^{--}), \pi_4(4^{-+}).
 \end{aligned} \tag{3}$$

The linearity of trajectories on the  $(n, M^2)$  plane (experimentally – up to large  $n$  values,  $n \leq 7$ ) gives us the  $t$ -channel singularity:  $V_{conf} \sim 1/q^4$  or, in the coordinate representation,  $V_{conf} \sim r$ . In the coordinate representation the confinement interaction can be written in the following potential form:

$$V_{conf} = (I \otimes I) b_S r + (\gamma_\mu \otimes \gamma_\mu) b_V r, \tag{4}$$

with  $b_S \simeq -b_V \simeq 0.15 \text{ GeV}^{-2}$ .

The spectral integral equation for the  $q\bar{q}$ -meson wave function was solved by introducing a cut-off into the interaction:  $r \rightarrow r e^{-\mu r}$ . The cut-off parameter is small,  $\mu \sim 1 - 10 \text{ MeV}$ .

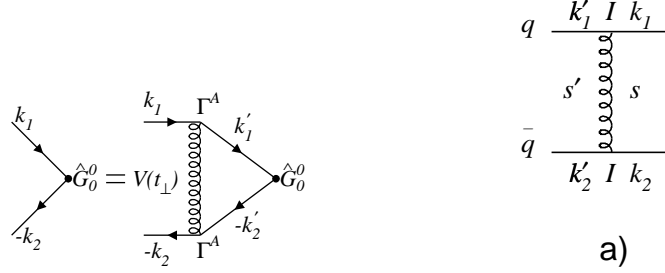


Figure 7: Spectral integral equation and interaction block

In general, keeping in mind that in the framework of spectral integral method (as in the dispersion technique) the total energy is not conserved, we have to write:

$$t_{\perp} = (k_1^{\perp} - k_1'^{\perp})_{\mu} (-k_2^{\perp} + k_2'^{\perp})_{\mu} . \quad (5)$$

Recall that  $k_1$  and  $k_2$  are momenta of the initial quark and antiquark, while  $k_1'$  and  $k_2'$  are those after the interaction. The index  $\perp$  means that we use components perpendicular to the total momentum  $p = k_1 + k_2$  for the initial state and to  $p' = k_1' + k_2'$  for the final state.

$$r^N e^{-\mu r} = \int \frac{d^3 q}{(2\pi)^3} e^{-i\vec{q}\vec{r}} I_N(t_{\perp}), \quad s = s', \quad \mu \sim \frac{1}{r_0}, \quad (6)$$

$$I_N(t_{\perp}) = \frac{4\pi(N+1)!}{(\mu^2 - t_{\perp})^{N+2}} \sum_{n=0}^{N+1} (\mu + \sqrt{t_{\perp}})^{N+1-n} (\mu - \sqrt{t_{\perp}})^n .$$

### 3.2 Simple example of the spectral integral equation: the pion state ( $J^{PC} = 0^{-+}$ )

$$\bar{\psi}(-k_2) i\gamma_5 g^{(0,0,0)}(s) \psi(k_1) = \int \frac{d^3 k'}{(2\pi)^3 k_0'} \bar{\psi}(-k_2) V(t_{\perp}) \Gamma^A (-\hat{k}_2' + m) \frac{i\gamma_5 g^{(0,0,0)}(s')}{s' - M^2} (\hat{k}_1' + m) \Gamma_A \psi(k_1) . \quad (7)$$

$$\hat{G}^{(0,0,0)}(k_{\perp}) = i\gamma_5, \quad \hat{\Psi}_n^{(0,0,0)}(s) = \hat{G}^{(0,0,0)}(k_{\perp}) \frac{g_n^{(0,0,0)}(s)}{s - M_n^2} = \hat{G}^{(0,0,0)}(k_{\perp}) \psi_n^{(0,0,0)}(s). \quad (8)$$

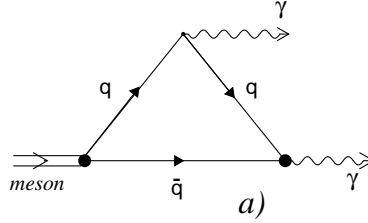


Figure 8: Two-photon decay of a meson

## 4 Two-photon decay of mesons

Considering radiative decays of hadrons in the spectral integral technique, we should take into account two subprocesses for the two-photon decay of a  $q\bar{q}$  state: the emission of a photon in the intermediate state by a quark (or an antiquark) and subsequent annihilation  $q\bar{q} \rightarrow \gamma$ .

### 4.1 Photon wave function

The photon wave function has two components: the soft and hard ones. The hard component is related to the point-like vertex  $\gamma \rightarrow q\bar{q}$ , it is responsible for the production of a quark–antiquark pair at high photon virtuality. The soft component is responsible for the production of low-energy quark–antiquark vector states such as  $\rho^0$ ,  $\omega$ ,  $\phi(1020)$  and their excitations.

The photon wave function for the  $q\bar{q}$  system reads:

$$\psi_{\gamma^*(Q^2) \rightarrow q\bar{q}}(s) = \frac{G_{\gamma \rightarrow q\bar{q}}(s)}{s + Q^2} . \quad (9)$$

The photon wave function has been found under the assumption of the vertex universality for  $u$  and  $d$  quarks,  $G_{\gamma \rightarrow u\bar{u}}(s) = G_{\gamma \rightarrow d\bar{d}}(s) \equiv G_{\gamma}(s)$ . It looks rather trustworthy because of the degeneracy trajectories of  $\rho$  and  $\omega$  states.

### 4.2 Transition form factors $\pi^0 \rightarrow \gamma^*(Q_1^2)\gamma^*(Q_2^2)$

In Fig. 9, one can see the results of the calculation of transition form factors  $\pi^0, \eta, \eta' \rightarrow \gamma(Q^2)\gamma$ , which appeared to be in a good agreement with experimental data.

Using the same technique as for the  $meson \rightarrow \gamma^*(Q^2)V$  amplitude, we can write the formulae for the transition form factors of the pseudoscalar mesons  $\pi^0, \eta, \eta' \rightarrow \gamma^*(Q_1^2)\gamma^*(Q_2^2)$ .

The general structure of the amplitude for these processes is as follows:

$$A_{\mu\nu}^{(P \rightarrow \gamma^* \gamma^*)}(Q_1^2, Q_2^2) = e^2 \epsilon_{\mu\nu\alpha\beta} q_\alpha p_\beta F_{(\pi, \eta, \eta') \rightarrow \gamma^* \gamma^*}(Q_1^2, Q_2^2) , \quad (10)$$

here  $q = (q_1 - q_2)/2$ ,  $p = q_1 + q_2$ ,  $q_i^2 = -Q_i^2$ .

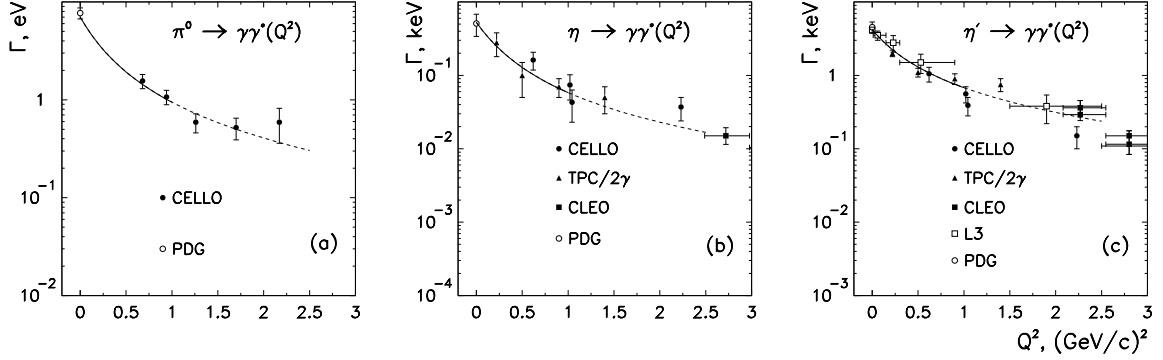


Figure 9: Data for  $\pi^0 \rightarrow \gamma\gamma^*$ ,  $\eta \rightarrow \gamma\gamma^*$ ,  $\eta' \rightarrow \gamma\gamma^*$  vs calculated curves.

In terms of the light-cone variables  $(x, \vec{p})$  the amplitude for the form factor  $\pi^0 \rightarrow \gamma^*(Q_1^2)\gamma^*(Q_2^2)$  reads:

$$F_{\pi \rightarrow \gamma^* \gamma^*}(Q_1^2, Q_2^2) = \zeta_{\pi \rightarrow \gamma\gamma} \frac{\sqrt{N_c}}{16\pi^3} \int_0^1 \frac{dx}{x(1-x)^2} \int d^2k_\perp \Psi_\pi(s) \times \left( S_{\pi \rightarrow \gamma^* \gamma^*}(s, s'_1, Q_1^2) \frac{G_{\gamma^*}(s'_1)}{s'_1 + Q_2^2} + S_{\pi \rightarrow \gamma^* \gamma^*}(s, s'_2, Q_2^2) \frac{G_{\gamma^*}(s'_2)}{s'_2 + Q_1^2} \right), \quad (11)$$

where  $s = (m^2 + k_\perp^2)/[x(1-x)]$ ,  $s'_i = [m^2 + (\mathbf{k}_\perp - x\mathbf{Q}_i)^2]/[x(1-x)]$ , ( $i = 1, 2$ ). and  $S_{\pi \rightarrow \gamma^* \gamma^*}(s, s'_i, Q_i^2) = 4m$ ,  $\zeta_{\pi \rightarrow \gamma\gamma} = (e_u^2 - e_d^2)/\sqrt{2} = 1/(3\sqrt{2})$ .

The factor  $\sqrt{N_c}$  appears owing to the definition of the colour wave function for the photon which differs from that for the pion: in the pion wave function there is a factor  $1/\sqrt{N_c}$  while in the photon wave function this factor is absent.

In terms of the spectral integrals over the  $(s, s')$  variables, the amplitude for  $\pi^0 \rightarrow \gamma^*(Q_1^2)\gamma^*(Q_2^2)$  reads:

$$F_{\pi \rightarrow \gamma^* \gamma^*}(Q_1^2, Q_2^2) = \zeta_{\pi \rightarrow \gamma\gamma} \frac{\sqrt{N_c}}{16} \int_{4m^2}^\infty \frac{ds}{\pi} \frac{ds'}{\pi} \Psi_\pi(s) \times \left[ \frac{\Theta(s'sQ_1^2 - m^2\lambda(s, s', -Q_1^2))}{\sqrt{\lambda(s, s', -Q_1^2)}} S_{\pi \rightarrow \gamma^* \gamma^*}(s, s', Q_1^2) \frac{G_{\gamma^*}(s')}{s' + Q_2^2} + \frac{\Theta(s'sQ_2^2 - m^2\lambda(s, s', -Q_2^2))}{\sqrt{\lambda(s, s', -Q_2^2)}} S_{\pi \rightarrow \gamma^* \gamma^*}(s, s', Q_2^2) \frac{G_{\gamma^*}(s')}{s' + Q_1^2} \right], \quad (12)$$

where  $\lambda(s, s', -Q_i^2) = (s - s')^2 + 2Q_i^2(s + s') + Q_i^4$ ,  $\Theta(X > 0) = 1$  and  $\Theta(X < 0) = 0$ .

In the radiative decays  $\rho, \omega \rightarrow \gamma\pi$  we face two mechanisms: a bremsstrahlung emission of a photon  $q \rightarrow \gamma + q$ , with a subsequent transition  $q\bar{q} \rightarrow \pi$ , and a bremsstrahlung-type emission of a pion  $q \rightarrow \pi + q$ , with a subsequent annihilation  $q\bar{q} \rightarrow \gamma$ .



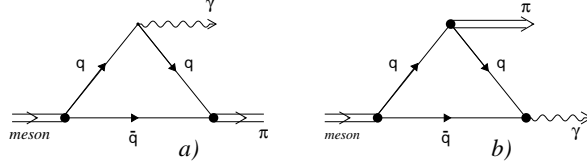


Figure 10: The  $\rho, \omega \rightarrow \gamma\pi$  decay

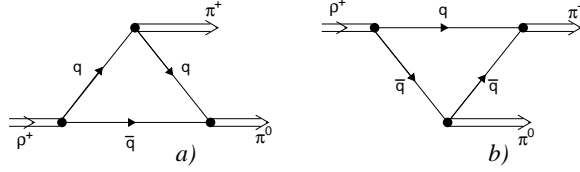


Figure 11: Decay  $\rho \rightarrow \pi\pi$ . These two diagrams, being taken into account only, result in  $\Gamma_{\rho(775) \rightarrow \pi\pi} \simeq 2000 \text{ MeV}$

The key point in the calculation of the  $\rho, \omega \rightarrow \gamma\pi$  decays is to know the  $q\bar{q}$  wave functions of the pion and vector mesons,  $\rho$  and  $\omega$ , as well as the wave function of the photon  $\gamma \rightarrow q\bar{q}$ . The pion bremsstrahlung constant for the process  $q \rightarrow \pi q$  is determined by the pion-nucleon coupling constant  $g_{\pi\pi N}^2/(4\pi) \simeq 14$ . We have calculated partial widths – they coincide with the observed ones:  $\Gamma_{\rho^\pm \rightarrow \gamma\pi^\pm}^{(exp)} = 68 \pm 30 \text{ keV}$ ,  $\Gamma_{\rho^0 \rightarrow \gamma\pi^0}^{(exp)} = 77 \pm 28 \text{ keV}$ ,  $\Gamma_{\omega \rightarrow \gamma\pi^0}^{(exp)} = 776 \pm 45 \text{ keV}$ .

## 5 Decay $\rho \rightarrow \pi\pi$

The study of  $\rho \rightarrow \pi\pi$  demonstrates us that in this decay, apart from the pion bremsstrahlung processes, we should include into consideration the Gribov quark exchange [13].

The Gribov's transition  $q\bar{q} \rightarrow \pi\pi$ , see Fig. 12c, is necessary for the numerical description of the  $\rho(775) \rightarrow \pi\pi$  decay width. However, the structure of the  $q\bar{q} \rightarrow \pi\pi$  amplitude is not determined unambiguously – there remains a freedom in choosing the singularity.

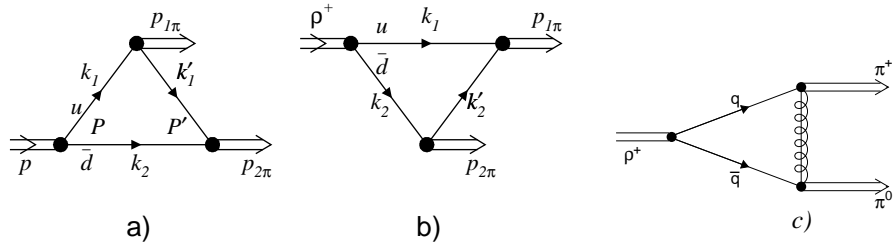


Figure 12: The  $\rho^+ \rightarrow \pi^+\pi^0$  process: a,b) with a bremsstrahlung-type pion emission and c) with the  $q\bar{q} \rightarrow \pi\pi$  transition, realized owing to the  $t$ -channel confinement singularity with fermion quantum numbers. These three diagrams give  $\Gamma_{\rho(775) \rightarrow \pi\pi} \simeq 150 \text{ MeV}$

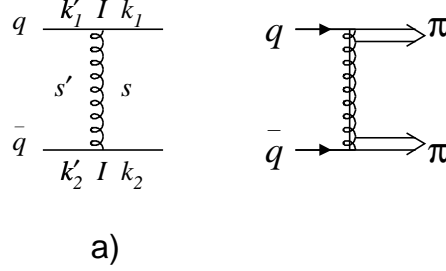


Figure 13: Confinement interactions: singular locking block and Gribov's quark exchange.

The estimate of the amplitude  $q\bar{q} \rightarrow \pi\pi$  for different interaction versions has been done in [14].

The calculation of amplitudes demonstrates that for the quark confinement principally decisive is the singular interaction:  $1/t_\perp^2$  – just because of this interaction the quark singularities are absent in the decay amplitudes. Correspondingly, the amplitudes are real in the physical region.

The Gribov's singularity plays another and very important role. The matter is that the bremsstrahlung-type radiation of pions (*i.e.* the radiation coming from the region of the confinement trap) is rather large. Were it the only possible process, it would lead to a broad decay width of the  $\rho$  meson,  $\sim 2000$  MeV. But the process with Gribov's singularity prevents such a “smearing”, – it looks like the only way for keeping the  $\rho$  meson as a comparatively narrow state.

## 5.1 Self-energy part $\rho \rightarrow \pi\pi \rightarrow \rho$

Up to now we neglect the reverse influence of the  $\pi\pi$  channel upon the characteristics of the  $\rho$  meson. To take it into account one needs to consider the two-channel ( $q\bar{q}$ ,  $\pi\pi$ ) equation, see Fig. 14.

A small value of the  $(\rho_{(q\bar{q})} \rightarrow \pi\pi)$  width allows us to simplify the equation of Fig. 14 – see Fig. 15. Then, we have a standard one-channel equation for  $\rho_{(q\bar{q})}$  where  $\rho_{(q\bar{q})}$  is a pure  $q\bar{q}$  state. The  $\pi\pi$  channel reveals itself in the self-energy part  $\rho_{(q\bar{q})} \rightarrow \pi\pi \rightarrow \rho_{(q\bar{q})}$ .

One can see that the self-energy part  $B(s, M_{\rho_{(q\bar{q})}}^2)$  determines the admixture of the  $\pi\pi$  component in the  $\rho$  meson, and the amplitude has hadron singularities only; quark cuttings give zero contributions.

Indeed, with this self-energy part,  $B(s, M_{\rho_{(q\bar{q})}}^2)$ , one transforms the propagator of a pure  $q\bar{q}$  state:

$$\frac{\sum_a \epsilon_\nu^{(a)} \epsilon_{\nu'}^{(a)+}}{M_{\rho_{(q\bar{q})}}^2 - s} \Rightarrow \frac{\sum_a \epsilon_\nu^{(a)} \epsilon_{\nu'}^{(a)+}}{M_{\rho_{(q\bar{q})}}^2 - s - B(s, M_{\rho_{(q\bar{q})}}^2)} = \quad (13)$$

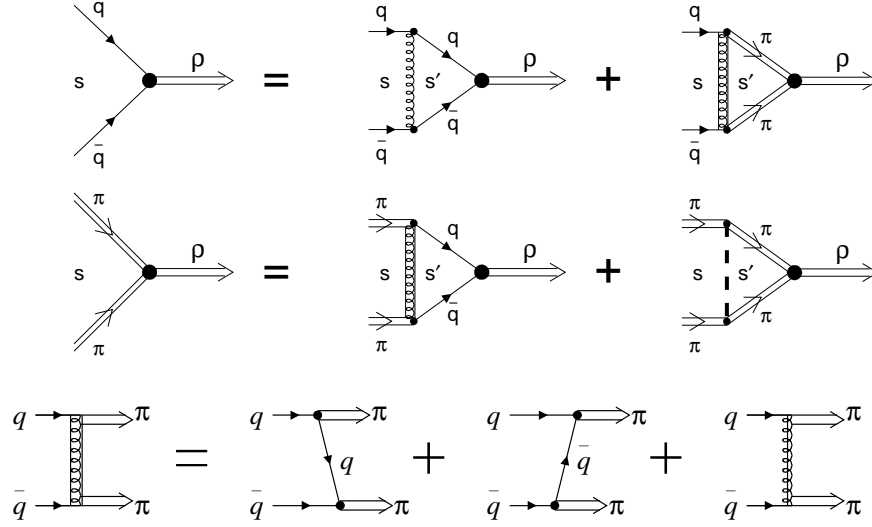


Figure 14: Two-channel  $(q\bar{q}, \pi\pi)$  equation: The following simplifying steps can be done: (i) The second term in the right-hand side of the  $(q\bar{q} \rightarrow \rho)$ -equation may be considered as a perturbative correction because the  $\rho$ -meson width is not large. (ii) The last term in the equation  $\pi\pi \rightarrow \rho$  can be neglected due to the smallness of the  $\pi\pi$  interaction in the  $\rho$ -meson region.

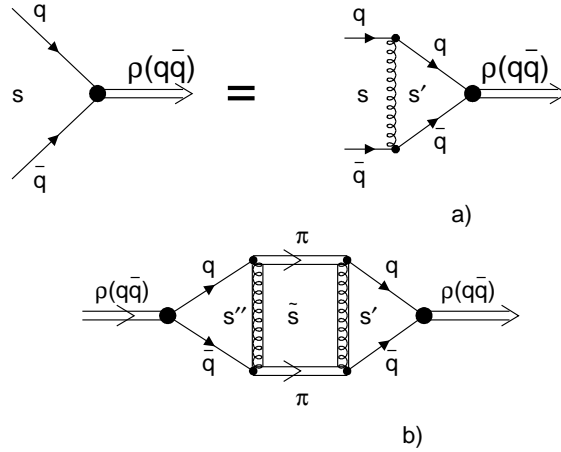


Figure 15: Standard  $q\bar{q}$  equation and the  $\rho$ -meson self-energy part  $\rho(q\bar{q}) \rightarrow \pi\pi \rightarrow \rho(q\bar{q})$ .

$$= \frac{\sum_a \epsilon_\nu^{(a)} \epsilon_{\nu'}^{(a)+}}{M_{\rho(q\bar{q})}^2 - \text{Re}B(s, M_{\rho(q\bar{q})}^2) - s - i \text{Im}B(s, M_{\rho(q\bar{q})}^2)} \simeq \frac{\sum_a \epsilon_\nu^{(a)} \epsilon_{\nu'}^{(a)+}}{M_\rho^2 - s - i M_\rho \Gamma_\rho},$$

where

$$\begin{aligned} M_\rho^2 &= M_{\rho(q\bar{q})}^2 - \text{Re} B(M_\rho^2, M_{\rho(q\bar{q})}^2) = (0.770)^2 \text{GeV}^2, \\ M_\rho \Gamma_\rho &= \text{Im} B(M_\rho^2, M_{\rho(q\bar{q})}^2). \end{aligned} \quad (14)$$

The fit tells us that  $M_\rho^2 \simeq M_{\rho(q\bar{q})}^2$ , thus providing us with a rather small value of the mass shift in the region of  $s \sim M_\rho^2$ :

$$\text{Re} B(M_\rho^2, M_{\rho(q\bar{q})}^2) \simeq 0. \quad (15)$$

## 5.2 Self-energy part $B(s, M_{\rho(q\bar{q})}^2)$ and confinement

The self-energy part of a pure  $q\bar{q}$  state reads:

$$\begin{aligned} B(s, M_{\rho(q\bar{q})}^2) &= \int_{4M_\pi^2}^{\infty} \frac{ds_{\pi\pi}}{\pi} \frac{\text{Im}B(s_{\pi\pi}, M_{\rho(q\bar{q})}^2)}{s_{\pi\pi} - s - i0}, \\ \text{Im}B(s_{\pi\pi}, M_{\rho(q\bar{q})}^2) &= \frac{1}{48\pi} \sqrt{\frac{(s_{\pi\pi} - 4M_\pi^2)^3}{s_{\pi\pi}}} [2A(\triangle_{\pi^0}^+; s_{\pi\pi}, M_\rho^2) + A(\triangle_{\pi^0}^+; s_{\pi\pi}, M_\rho^2)]^2. \end{aligned} \quad (16)$$

We should emphasize that the self-energy amplitude, despite the presence of the quark–antiquark state in intermediate states, have no corresponding imaginary part. This means the quark confinement. The only particles flying away are pions: the threshold singularity in the amplitude manifests just this fact.

## 6 Conclusion

The equations for  $q\bar{q}$  mesons, which are constructed in terms of dispersion relation technique (or spectral integral technique), are in certain respect similar to Schrödinger equations with infinite potential barrier. Spectral integral equations, taking into account the relativism of constituents, make it possible to describe the confined  $q\bar{q}$  systems and to calculate meson masses and  $q\bar{q}$  wave functions. For the quark confinement, principally crucial are singular interactions [1].

Singular interactions, imposing the confinement trap constraints, allow us to calculate the radiative decay amplitudes and widths:  $(q\bar{q})_{in} \rightarrow \gamma^* \rightarrow e^+e^-$ ,  $(q\bar{q})_{in} \rightarrow \gamma\gamma$ ,  $(q\bar{q})_{in} \rightarrow \gamma(q\bar{q})_{out}$ .

A special treatment is needed for reactions with the production of  $\gamma\pi$  and two-pion decay. Here we face the bremsstrahlung-type emission of pions (*i.e.*, the emission coming from the region of the confinement trap). Besides, in the two-pion production,  $\rho \rightarrow \pi\pi$ , a special type of singular interaction must exist, namely, Gribov’s singularity – it prevents a “smearing” of the  $\rho$  meson.

So, the calculations tell us that in terms of the dispersion relation technique we need three types of diagrams for the description of the transition  $q\bar{q} \rightarrow \pi\pi$ : with the emission of a pion by quark, antiquark, and a simultaneous production of two pions that plays a role of a subtraction term in the interaction block.

The calculation of the self-energy part  $\rho \rightarrow \pi\pi \rightarrow \rho$  demonstrates that the model of constituent quarks, in its standard version presented here, does not leave a room for the inclusion of the pion cloud into consideration. Indeed, along with pion cloud component, it is necessary to decrease the size and mass of the " $q\bar{q}$  bag" ( $R_{q\bar{q}\text{-bag}}^2 < R_{\rho\text{-meson}}^2$ ), *i.e.*, it is necessary to change the logic of spectral integral equations for mesons.

I thank L.G. Dakhno and M.A. Matveev for useful comments.

## References

- [1] A.V. Anisovich, V.V. Anisovich, J. Nyiri, V.A. Nikonov, M.A. Matveev and A.V. Sarantsev, *Mesons and Baryons. Systematization and Methods of Analysis*, World Scientific, Singapore, 2008.
- [2] A.V. Anisovich, V.V. Anisovich, and A.V. Sarantsev, Phys. Rev. D **62**:051502(R) (2000).
- [3] A.V. Anisovich, C.A. Baker, C.J. Batty, *et al.*, Phys. Lett. B **449**, 114 (1999); B **452**, 173 (1999); B **452**, 180 (1999); B **452**, 187 (1999); B **472**, 168 (2000); B **476**, 15 (2000); B **477**, 19 (2000); B **491**, 40 (2000); B **491**, 47 (2000); B **496**, 145 (2000); B **507**, 23 (2001); B **508**, 6 (2001); B **513**, 281 (2001); B **517**, 261 (2001); B **517**, 273 (2001); Nucl. Phys. A **651**, 253 (1999); A **662**, 319 (2000); A **662**, 344 (2000).
- [4] V.A. Shchegelsky, A.V. Sarantsev, A.V. Anisovich and M.P. Levchenko, Eur. Phys. J. A **27** (2006) 199.
- [5] V.V. Anisovich and A.V. Sarantsev, Phys. Lett. B **382**, 429 (1996); V.V. Anisovich, D.V. Bugg and A.V. Sarantsev, Yad. Fiz. **62**, 1322 (1999) [Physics of Atomic Nuclei **62**, 1247 (1999)]; V.V. Anisovich, A.A. Kondashov, Yu.D. Prokoshkin, S.A. Sadovsky, and A.V. Sarantsev, Yad. Fiz. **60**, 1489 (2000) [Phys. Atom. Nucl. **60**, 1410 (2000)], hep-ph/9711319.
- [6] V.V. Anisovich and A.V. Sarantsev, Eur. Phys. J. A **16**, 229 (2003); JETP Letters **81**, 417 (2005); Yad. Fiz. **72**, 1950 (2009) [Phys. At. Nucl., **72**, 1889 (2009)]; Yad. Fiz. **72**, 1981 (2009) [Phys. At. Nucl., **72**, 1920 (2009)]; Int. J. Mod. Phys. A **24**, 2481 (2009);
- [7] A.V. Anisovich, V.V. Anisovich, Yu.D. Prokoshkin, and A.V. Sarantsev, Zeit. Phys. A **357**, 123 (1997); A.V. Anisovich, V.V. Anisovich, and A.V. Sarantsev, Phys. Lett. B **395**, 123 (1997); Zeit. Phys. A **359**, 173 (1997).

- [8] V.V. Anisovich, UFN, **174**, 49 (2004) [Physics-Uspekhi, **47**, 45 (2004)].
- [9] V.V. Anisovich, Pis'ma JETP **80**, 845 (2004) [JETP Letters **80**, 715 (2004)];  
V.V. Anisovich and A.V.Sarantsev, Pis'ma JETP **81**, 531 (2005) [JETP Letters **81**, 417 (2005)];  
V.V. Anisovich and A.V.Sarantsev, V.V. Anisovich, J. Nyiri, M.A. Matveev and A.V.Sarantsev, Int. J. Mod. Phys. A **20**, 6327 (2005).
- [10] V.V. Anisovich, L.G. Dakhno, M.A. Matveev, V.A. Nikonov, and A. V. Sarantsev, Yad. Fiz. **70**, 68 (2007) [Phys. Atom. Nucl. **70**, 63 (2007)];  
Yad. Fiz. **70**, 392 (2007) [Phys. Atom. Nucl. **70**, 364 (2007)],  
Yad. Fiz. **70**, 480 (2007) [Phys. Atom. Nucl. **70**, 450 (2007)].
- [11] V.V. Anisovich, D.I. Melikhov and V.A. Nikonov, *Phys. Rev. D* **52**, 5295 (1995);  
A.V. Anisovich, V.V. Anisovich, L.G. Dakhno, V.A. Nikonov, and V.A. Sarantsev, Yad. Fiz. **68**, 1892 (2005) [Phys. Atom. Nucl. **68**, 1830 (2005)].
- [12] R. Briere, *et al.* (CLEO Collab.), Phys. Rev. Lett. **84**, 26 (2000),  
M. Acciarri, *et al.* (L3 Collab.), Phys. Lett. B **501**, 1 (2001); B **418**, 389 (1998);  
L. Vodopyanov *et al.* (L3 Collab.), Nucl. Phys. Proc. Suppl. **82**, 327 (2000),  
H.J. Behrend, *et al.* (CELLO Collab.), Z. Phys. C **49**, 401 (1991),  
H. Aihara, *et al.* (TRC/ $2\gamma$  Collab.), Phys. Rev. D **38**, 1 (1988).
- [13] V.N. Gribov, "Theory of Quark Confinement", World Scientific, Singapore, (2001)
- [14] A.V. Anisovich, V.V. Anisovich, L.G. Dakhno, M.A. Matveev, V.A. Nikonov, and A. V. Sarantsev, J. Phys. G: Nucl. Part. Phys. **37**, 025004 (2010);  
Yad. Fiz. **73**, 444 (2010) [Phys. Atom. Nucl. **73**, 462 (2010)].

